Journal of Optoelectronics and Advanced Materials Vol. 7, No. 4, August 2005, p. 2001 - 2011

# THE LIQUID STRUCTURE OF CdTe ALLOY USING THE AMEAM POTENTIALS

S. Senturk Dalgıc[a,b,*], S. Sengul[a], S. Kalaycı[a]

[a]Department of Physics, Trakya University, 22030 Edirne, Turkey
[b]International Center for Physics and Applied Mathematics, Trakya University, P.K.126, 22030 Edirne, Turkey

The structure of molten cadmium telluride have been calculated using the integral equation theories with the efective pair potentials based on the analytic modified embedded atom method (AMEAM). The pair interactions are described with the semi-empirical potential functions recently proposed Hu and co-workers. All the potential parameters for pure components are determined by fitting both liquid and solid state properties. The structural properties of liquid Cd-Te equiatomic alloy have been obtained using the Variational Modified Hypernetted Chain liquid state theory. The results of partial pair distribution functions are compared with the neutron diffraction data and those obtained by Stillinger-Weber semi-empirical potential.

(Received July 4, 2005; accepted July 21, 2005)

*Keywords:* Cadmium telluride, Liquid structure, Analytic modified embedded atom method, Stillinger-Weber potential

## 1. Introduction

One of the basic concepts to understand the properties of the materials is the atomic interactions. Most semi-empirical or empirical descriptions of atomic interactions based on the embedded atom method (EAM) have been developed. The EAM potentials proposed by Daw and Baskes [1] and the long range EAM potentials introduced by Finnis and Sinclair (FS) [2] give more realistic description of material properties than can be obtained by pair potentials. However, empirical pair potential interactions between atoms which have been used in computer simulation studies are less common for hcp metals than cubic metals because of obtaining suitable interatomic potentials. The many body potentials for hcp metals was proposed by Johnson and co-workers [3-5] and Ackland [6,7]. Baskes and Johnson [8] developed a modified EAM potential (MEAM) for hcp metals. The modified EAM potentials proposed by Baskes and Johnson [8] with angular forces were applied to eighteen hcp metals, including hcp rare-earth metals. They studied the vacancy, divacancy, stacking fault and surface properties. Pasianot et al.[9] add a modified analytic energy term M(P) to the total energy expression for the EAM which was defined in realting the angular momentum contributions to the background electron densities and the atom densities. Thus the M(P) term can be defined as the difference between the actual total energy of atoms and the calculated from original EAM using a linear superposition of spherical densities of atomic electrons. Related to this, Hu and co-workers [10] have proposed an analytic EAM potential (AEAM) for hcp metals. They added one another energy modification term in the total energy expression in a familiar way just as Pasianot *et.al* [9] did. Two parameters $\alpha$ and $\beta$ that describe the anisotropy of hcp structure were added. Contrast to some researchers who considered the angular forces and screening effects of atoms in outer shells by atoms in inner shells [11] a different way of thought, a new scheme of EAM potential for hcp metals was given by Chen *et.al.*[12].

On the other hand, based on those previous studies, Hu and co-workers [13] have constructed a new analytic modified EAM many-body potential (AMEAM) for hcp metals currently, and calculated the thermodynamic properties of Mg-RE alloys [14]. These potentials have been

*Corresponding author: serapd@trakya.edu.tr

applied for hcp rare-earth metals and properties of various defects have been evaluated [15]. They have shown that these potentials reproduce exactly the observed *c/a* ratio and all five elastic constants for each metal considered. According to our knowledge, there is no reported work about the applicability of these potentials for chalcogenide metals. In the present work, the potential functions of the AMEAM proposed by Hu and co-workers [10, 13, 14, 15] have been used to obtain the liquid structure of hcp chalcogenide metals and metal alloys. The Cd and Te metals and CdTe metal alloys have been chosen as a test case.

It is known that the liquid Te has metallic properties while the solid Te is an typical semiconductor. Besides being a technologically important compound, liquid CdTe (l-CdTe) also presents an interesting subject for fundamental studies [16-19]. CdTe is among those II-VI semiconductors that, in liquid phase, exhibit properties which are fundamentally different from those of liquid IV and III-V semiconductors [16]. The semiconductor behaviour of l-CdTe was observed only in a narrow temperature range immediately after melting temperature [17, 18] In particular, neutron-scattering experiments [18] have suggested that the liquid CdTe conserves its crystalline open structure environment with coordination number of ~4. A number of studies have been reported the semi-empirical potential calculations for CdTe. Wang *et.al.*[19] have modelled the stoichiometric compound of CdTe by the empirical two-body and three-body Stillinger-Weber (SW) potentials [20] in order to investigate both bulk and surface properties by the Monte Carlo (MC) method. Recently, Glazov *et.al* [21] have calculated the structural characteristics of molten CdTe using the molecular dynamics (MD) simulation method with the use of a SW empirical potential.

In this work, we have also used the semi-empirical many-body potentials such as those based on the EAM. The AMEAM potential functions for Cd, Te and CdTe have been parameterized which give a good description of their liquid and still describe the solid states accurately. The effective interatomic interactions are modelled by a combination of the AMEAM potential functions with improving of the Finnis-Sinclair (FS) effective potential approximation based on the EAM [2]. The constructed effective potentials are used as input data in our structural calculations. The static structure factors for pure metals and partial structure factors and pair distribution functions are calculated with one of the integral equation theory of liquids namely, variational modified hypernetted chain (VMHNC) theory [22-24] which was successfully applied to metallic systems in the EAM calculations [25-28]. The VMHNC results are compared with available experimental data and MD results to determine the reliability of the AMEAM for describing the structural properties of liquid Cd, Te and CdTe systems.

## 2. Theory

### 2.1 Effective pair potentials

The total energy of atomic structure for hcp metals can be expressed as the sum of four terms, a many-body term, which depends on the local electron density, a two-body term, which depends on the interatomic distances, and two modification terms to correct the discrepancy from the assumption of the linear superposition of spherical atomic electron density in the original EAM:

In the AMEAM, the basic equation of the total energy of a system of atoms is given by

$$E_{total} = \sum_i F(\rho_i) + \frac{1}{2}\sum_i \sum_{\substack{j \\ i \neq j}} \phi(r_{ij}) + \sum_i M(P_i) + \sum_i N(Q_i)\,. \tag{1}$$

The energy modification terms $M(P_i)$ and $N(Q_i)$ are empirically taken as

$$M(P_i) = \alpha\left\{1 - \exp\left[-10000\left(\ln\left(\frac{P_i}{P_e}\right)\right)^2\right]\right\} \tag{2}$$

$$N(Q_i) = \beta\left\{1 - \exp\left[-10000\left(\ln\left(\frac{Q_i}{Q_e}\right)\right)^2\right]\right\} \tag{3}$$

where $P_e$ and $Q_e$ are their equilibrium values, α and β are taken as adjustable parameters. The host electron density $\rho_i$ induced at site i by all other atoms in the system is taken in the original form

$$\rho_i = \sum_j f(r_{ij}) \tag{4}$$

The arguments of the energy modification terms are taken as

$$P_i = \sum_j f^2(r_{ij}) \tag{5}$$

$$Q_i = \sum_j f^3(r_{ij}) . \tag{6}$$

The only one electron density function is used [13] in this defined as

$$f(r_{ij}) = f_e \left( \frac{r_{1e}}{r_{ij}} \right)^{4.5} \left( \frac{r_{ce} - r_{ij}}{r_{ce} - r_{1e}} \right)^2 \tag{7}$$

where the subscript e indicates equilibrium, $r_{1e}$ is the value of the nearest neighbour distance at equilibrium and $r_{ce}$ is the cutoff value at equilibrium. The parameter $f_e$ is the electron density scaling factor which can be determined from $f_e = \sqrt{E_c}/\Omega$ which is given as in Ref.[14]. Ω is the atomic volume. The embedding function $F(\rho_i)$ takes the same form as those used by Oh and Johnson [4]:

$$F(\rho_i) = -F_0 \left[ 1 - n \ln \left( \frac{\rho_i}{\rho_e} \right) \right] \left( \frac{\rho_i}{\rho_e} \right)^n \tag{8}$$

where $F_0 = E_c - E_{1f}$. $E_c$ is the cohesive energy and $E_{1f}$ is the unrelaxed vacancy formation energy of metal. $\rho_e$ takes its equilibrium value and can be determined from $\rho_e = 12 f_e$ as Ref. [29] for hcp metals. n is an another adjustable parameter.

The pair potential, $\phi(r_{ij})$ between atoms i and j with seperation distance $r_{ij}$ is taken as:

$$\phi(r_{ij}) = \sum_{m=-1}^{6} k_m \left( \frac{r_{ij}}{r_{1e}} \right)^m . \tag{9}$$

In the present model, the atomic interactions up to $r_c$ distance are considered. If the distance larger than or equal to $r_c$ and $r_{ce}$ the pair potential, electron density functions and their slopes go to zero. This is given as the two cut-off condition:

$$\phi(r_c) = 0, \quad \phi'(r_c) = 0; \qquad f(r_{ce}) = 0, \quad f'(r_{ce}) = 0 \tag{10}$$

An equation for the cohesive energy $E_c$ is taken as:

$$-E_c = \frac{1}{2} \sum \phi(r_c) - F_o \tag{11}$$

The parameters α, β and n can be determined from

$$E_{EOS}(a^*) = \frac{1}{2} \sum \phi(r_c) + F(\rho_c) + M(P_c) + N(Q_c) \tag{12}$$

where $E_{EOS}(a^*)$ is the Rose's equation of state [30] for the cohesive energy and a* is the reduced lattice constant. Overall this parameterization scheme for liquid hcp metals includes 11 free fitting parameters. The physical properties are fitted within this scheme to the cohesive energy, $E_c$, mono-vacancy formation energy, $E_{1f}$, and the two lattice constants of hexagonal structure a and c.

In order to construct the effective interatomic pair potential from the AMEAM, second and higher derivatives of the embedding function F are ignored. Thus we propose a new effective pair potential, $\phi_{eff}(r)$, form based on the Finnis–Sinclair (FS) approximation [2] for the AMEAM calculations. For pure metals, it takes as

$$\phi_{eff}(r) = \phi(r) - 2F'(\rho)\big(M(P) + N(Q)\big) f(r) . \tag{13}$$

For binary alloys, it can be defined as

$$\phi_{eff}^{AB}(r)=\phi_{AB}(r)-2F'_{AB}(\rho)(M_{AB}(P_{AB})+N_{AB}(Q_{AB}))f_{AB}(r) \tag{14}$$

where F′(ρ) is the first derivative of the embedding function. The alloy pair potential $\phi_{AB}(r)$ between different atomic species is taken as Johnson's formula [31]:

$$\phi^{AB}(r)=\frac{1}{2}\left[\frac{f^{B}(r)}{f^{A}(r)}\phi^{AA}(r)+\frac{f^{A}(r)}{f^{B}(r)}\phi^{BB}(r)\right]. \tag{15}$$

where AA and BB indicate A and B type atoms in a binary alloy. $\phi_{AA}(r)$ and $\phi_{BB}(r)$ are the monatomic potentials given by Eq. (9). The electron density function and modification terms for the alloy are taken as:

$$f_{AB}(r)=f_{e\,AB}\left(\frac{r_{1e\,AB}}{r}\right)^{4.5}\left(\frac{r_{ce\,AB}-r_{ij}}{r_{ce\,AB}-r_{1e\,AB}}\right)^{2}, \tag{16}$$

$$M_{AB}(P_{AB})=\alpha_{AB}\left\{1-\exp\left[-10000\left(\ln\left|\frac{P_{AB}}{P_{e\,AB}}\right|\right)^{2}\right]\right\}, \tag{17}$$

$$N_{AB}(Q_{AB})=\beta_{AB}\left\{1-\exp\left[-10000\left(\ln\left|\frac{Q_{AB}}{Q_{e\,AB}}\right|\right)^{2}\right]\right\}, \tag{18}$$

where

$$P_{AB}=\sum_{j}f_{AB}^{2}(r_j), \tag{19}$$

$$Q_{AB}=\sum_{j}f_{AB}^{3}(r_j). \tag{20}$$

The model parameters needed to calculate the effective potential of the alloy are evaluated from

$$\Gamma_{AB}=c\Gamma_{A}+(1-c)\Gamma_{B}.$$

where c is a concentration, $\Gamma_A$ and $\Gamma_B$ denotes the parameters of required potential functions for A and B metals i.e. $f_e$, n, $F_o$, α, β, $P_e$, $Q_e$..., $\Gamma_{AB}$ indicate the model parameters of alloy effective potential.

In this work, an alternative potential, proposed by Stillinger-Weber empirical potential (SW) [20] is used in alloy calculations:

$$\phi(r)=\begin{cases}\varepsilon\lambda\left(\kappa r^{-4}-1\right)\exp\left((r-\delta)^{-1}\right) & r<\delta\\ 0 & r\geq\delta\end{cases} \tag{21}$$

where ε, δ, κ and λ are adjustment potential parameters.

### 2.2 The VMHNC theory of liquids

With the effective pair potential known, integral equations are able to provide us the liquid structure for metals and alloy. In our structural calculations, one of the integral equation theories which have shown very reliable theory of liquids VMHNC has been carried out [22-24]. Like most liquid state theories the VMHNC solves the Ornstein – Zernike (OZ) equation for binary system reads (i, j =1, 2)

$$h_{ij}(r)=c_{ij}(r)+\sum_{l=1}^{2}\rho_l h_{il}(r)*c_{lj}(r) \tag{22}$$

which defines the partial direct correlation functions, $c_{ij}(r)$, in terms of the total correlation functions $h_{ij}(r)=g_{ij}(r)-1$, where $g_{ij}(r)$ denote the partial pair distribution functions and $\rho_l$ denote the partial ionic number densities. Now, Eq. (22) is solved by the exact closure relation

$$c_{ij}(r)=h_{ij}(r)-\ln\left[g_{ij}(r)e^{\beta\phi_{ij}(r)+B_{ij}(r)}\right] \tag{23}$$

where $\phi_{ij}(r)$ are the interatomic pair potentials and the $B_{ij}(r)$ denotes the PY bridge functions for binary system. The partial pair distribution functions are related to the partial structure factors $S_{ij}(q)$ by

$$g_{ij}(r)=1+\frac{1}{8\pi^3(\rho_i\rho_j)^{1/2}}\int(S_{ij}(q)-\delta_{ij})\exp(iqr)dq \tag{24}$$

## 3. Results and discussions

### 3.1. Simple liquid metals

We have calculated the effective pair potentials based on AMEAM potential functions for liquid hcp Cd and Te. The pair potenatial calculations are performed at T = 923 K for Cd and T = 823 K for Te, very near melting temperatures of Cd and Te. The number densities at these temperatures are evaluated by extrapolating of the empirical formula [32] which gives the temperature dependence of density for liquid metals and alloys linearly. The all parameters are determined by not only fitting to solid but also liquid state properties given in Table 1. The values of $r_c$ are determined by the procedure given in Eq.(10). The values of $E_c^{sol}$, $a^{sol}$ and $c^{sol}$ have been taken from Kittel [33]. The values of $r_{1e}$ are determined from experimental pair distribution function as the position of the first peak. In our liquid state calculations, we have calculated the liquid cohesive energy, $E_c^{liq}$ using the Rose's equation of state [30] and given in Table 1. We have determined the liquid parameters of the AMEAM potential functions by combining the two equations (Eq. 10) for the cut off condition, the equation for the cohesive energy (Eq. 11), the equation of the equilibrium condition (Eq. 12) and minimizing the configurational Helmholtz free energy. The reader is referred to our earlier work [28] for liquid state parametrization in the EAM based calculations.

Table 1. The parameters for liquid Cd and Te used in AMEAM calculations.

| Input parameters | | | Potential parameters | | |
|---|---|---|---|---|---|
| Parameter | Cd | Te | Parameter | Cd | Te |
| T(K) | 923 | 823 | $r_c$ (Å) | 5.13 | 5.12 |
| $\rho$(at./Å$^3$) | 0.04076 | 0.02703 | $r_{1e}$ (Å) | 3.00 | 3.00 |
| $E_c^{liq}$(eV) | 1.110 | 2.180 | $k_{-1}$ (eV) | 21.504 | 42.491 |
| $E_c^{sol}$(eV) | 1.160 | 2.190 | $k_0$ (eV) | -94.588 | -186.900 |
| $a^{liq}$(Å) | 3.100 | 4.000 | $k_1$ (eV) | 176.189 | 348.139 |
| $a^{sol}$(Å) | 2.980 | 3.880 | $k_2$ (eV) | -181.270 | -358.179 |
| $F_o$(eV) | 0.743 | 1.455 | $k_3$ (eV) | 111.618 | 220.552 |
| n | 0.520 | 0.480 | $k_4$ (eV) | -41.195 | -81.399 |
| $\alpha$(eV) | 0.2357 | 0.5185 | $k_5$ (eV) | 8.440 | 16.677 |
| $\beta$(eV) | -0.0394 | -0.0866 | $k_6$ (eV) | -0.740 | -1.462 |

The calculated embedding functions and the effective pair potentials using the AMEAM are shown in Figs. 1a and 1b for liquids Cd and Te, respectively. From Cd to Te in the same row of the periodic table, the obtained embedding energy gets deeper and wider and the position of the minimum towards to larger r values.

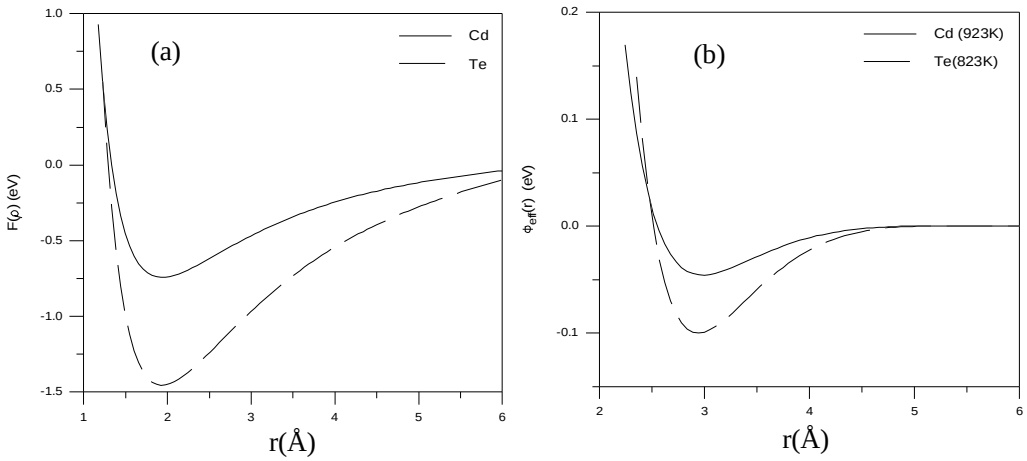


Fig. 1. (a) The calculated AMEAM embedding functions and (b) the effective pair potentials for liquids Cd and Te.

The similar results are observed for the effective pair potential presently shown in Fig. 1b. As it is seen that these potentials give the correct trend as far as the position of the concerned. As goes from Cd to Te in periodic table, the calculated potential becomes harder and the width increases. The presently obtained AMEAM effective pair potentials for Cd and Te are used as input data in our structural calculations. Calculated structure factors for liquid Cd and Te are shown in Fig. 2 together with the experimental data of Glazov [21]. It is noticed that the calculated and experimental structure factors differ in depth of the first minimum. We also find that the oscillations in the calculated structure factors S(q) die out more rapidly than in the experimental data.

In the case of Cd, as shown in Fig. 2a, the presented structure factor has a principal peak located at the same position of the experimental one. But for Te, the calculated main peak is somewhat shifted to larger r values in comparison with the experiment. After that the second maxima, the agreement with experiment is better.

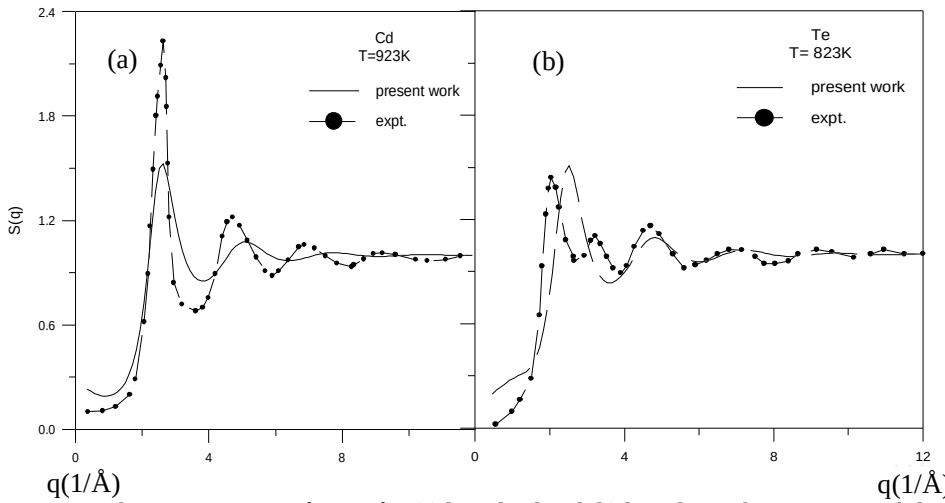


Fig. 2. The static structure factors for (a) liquid Cd and (b) liquid Te. The experimental data are taken from Ref. [21].

In Fig. 3, the calculated pair distribution functions, g(r), using the AMEAM potentials, for liquid Cd and Te are also compared with the experimental data which are available in the literature [34].

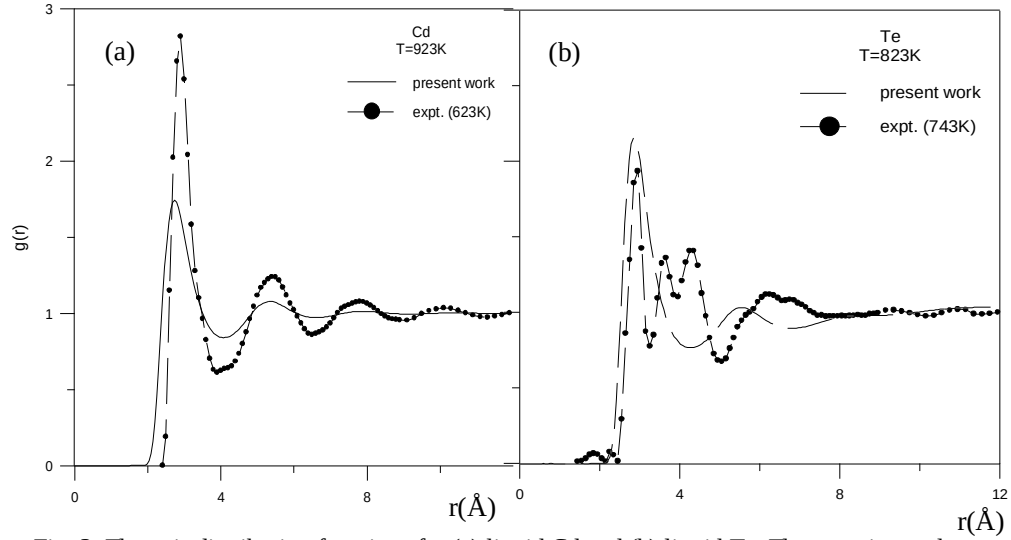


Fig. 3. The pair distribution functions for (a) liquid Cd and (b) liquid Te. The experimental data are taken from Ref. [34].

In contrast to the Te, the height of the calculated main peak of g(r) for Cd is underestimated. The main peak positions of g(r) are good agreement with experimental ones. In the case of Cd, the phases of oscillations in the calculated g(r) are in good agreement with experiment

### 3.2 Liquid binary CdTe alloy

We have also calculated the effective pair potentials based on the AMEAM potential functions for liquid CdTe alloys. All calculations are performed at T = 1373 K, very near the melting temperatures of CdTe alloy. The input parameters given in Table 2 are determined by fitting procedure mentioned in previous section.

Table 2. The parameters for liquid CdTe alloy used in AMEAM calculations.

| Input parameters | | | Potential parameters | | |
|---|---|---|---|---|---|
| Parameter | Cd | Te | Parameter | Cd | Te |
| T(K) | 1373 | | $r_c$ (Å) | 5.13 | 5.12 |
| $\rho_{alloy}$(at./ Å$^3$) | 0.02715 | | $r_{1e}$ (Å) | 3.00 | 3.00 |
| $E_c^{liq}$(eV) | 0.572 | 2.180 | $k_{-1}$ (eV) | 11.023 | 42.430 |
| $E_c^{sol}$(eV) | 1.160 | 2.190 | $k_0$ (eV) | -48.485 | -186.635 |
| $a^{liq}$(Å) | 3.560 | 4.000 | $k_1$ (eV) | 90.314 | 347.645 |
| $a^{sol}$(Å) | 2.980 | 3.880 | $k_2$ (eV) | -92.919 | -357.670 |
| $F_o$(eV) | 0.381 | 1.452 | $k_3$ (eV) | 57.215 | 220.239 |
| n | 0.41 | 0.51 | $k_4$ (eV) | -21.116 | -81.284 |
| α(eV) | 0.1644 | 0.4711 | $k_5$ (eV) | 4.326 | 16.654 |
| β(eV) | -0.0275 | -0.0787 | $k_6$ (eV) | -0.379 | -1.460 |

We have calculated the effective pair potentials for liquid CdTe using the SW empirical two-body potential. The potential parameters listed in Table 3 are taken from [19] where the λ and κ parameters were chosen so as to give the correct atomization energy and to satisfy the zero-pressure

condition for these imaginary structures at the correct nearest neighbour separation. The other parameters for SW potential are taken as $\varepsilon$ = 1.02 eV and $\delta$ = 1.80 [19].

Table 3. The SW two-body potential parameters for liquid CdTe.

| Metal | CdCd | CdTe | TeTe |
|---|---|---|---|
| $\lambda$ | 5.1726 | 7.0496 | 8.1415 |
| $\kappa$ | 0.8807 | 0.6022 | 0.6671 |

The calculated effective alloy potentials presently determined from the SW and AMEAM for equiatomic liquid CdTe alloy are shown in Figs. 4a and 4b, respectively.

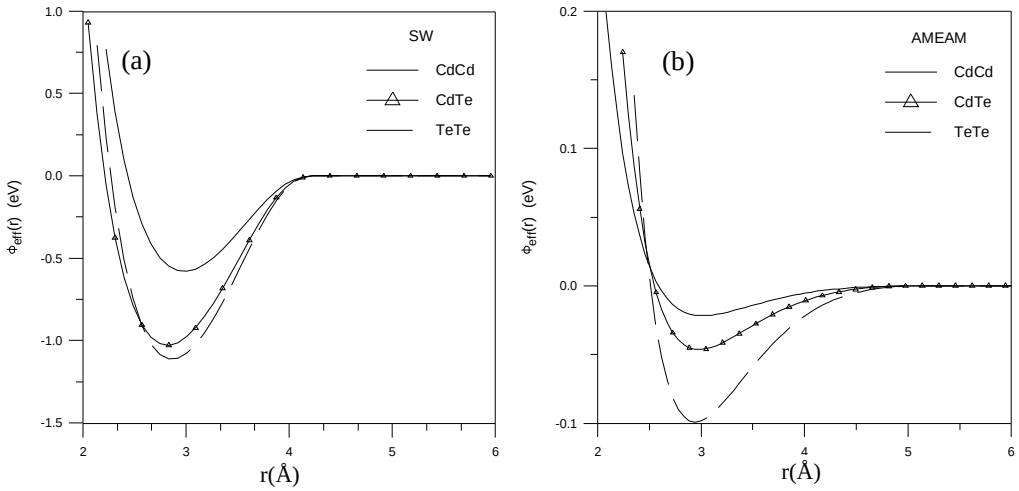


Fig. 4. Effective pair potentials $\phi_{eff}(r)$ determined from (a) SW and (b) AMEAM potentials for liquid CdTe.

It appears in these figures that the SW effective potential gives rise to a deep potential well, while the AMEAM yields a shallow well whereas both of the minima positions of potentials are in same r values. However, we have noted that the both calculated effective potentials show same correct trends as in pure metal calculations. In the structural calculations, partial pair correlation functions and partial structure factors have been calculated by constructed effective pair potentials for liquid equiatomic Cd-Te alloy. The Ashcroft-Langreth (AL) [35] description for the partial structure factors is used in conjunction with VMHNC. In Figs. 5a and 5b, we have presented the calculated partial pair correlation functions, $g_{ij}(r)$, using the SW and AMEAM potentials, compared with other available theoretical results those obtained from MD simulations based on the SW potential [19,21]. In Fig. 5b, contrast to Cd-Cd interactions in Cd-Te alloy, there is a good agreement in the first peak positions of Cd-Te and Te-Te between the presented and MD results. It suggests that our AMEAM calculations reproduce the angular dependent potential namely SW on the long range scale. To draw more definite conclusions on the structural state of the components in molten CdTe, the partial structure factors and partial pair correlation functions obtained by the AMEAM calculations are compared with the experimental data and those obtained by others in Fig. 6a and 6b.

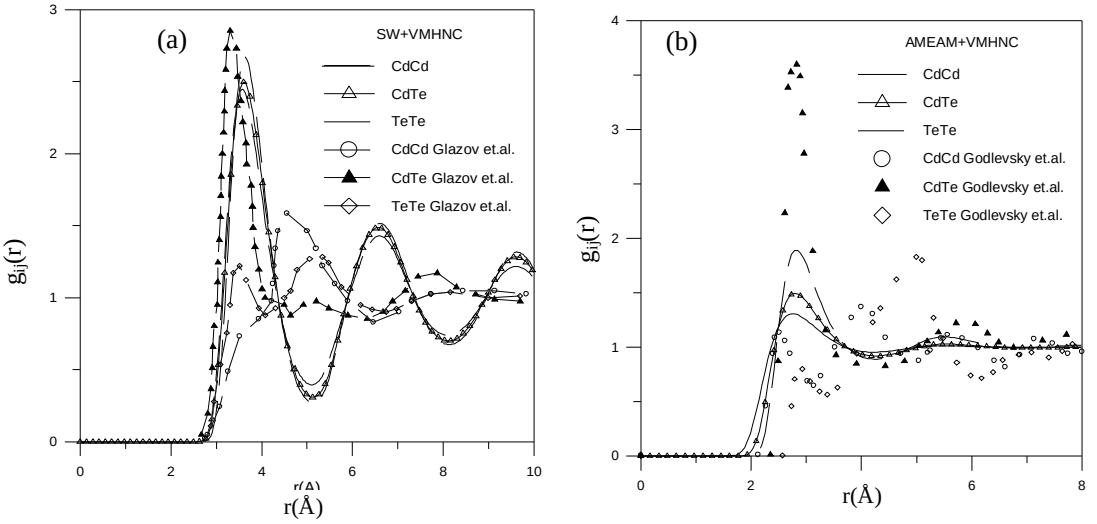


Fig. 5. Partial distribution functions obtained from (a) SW and (b) AMEAM potentials.

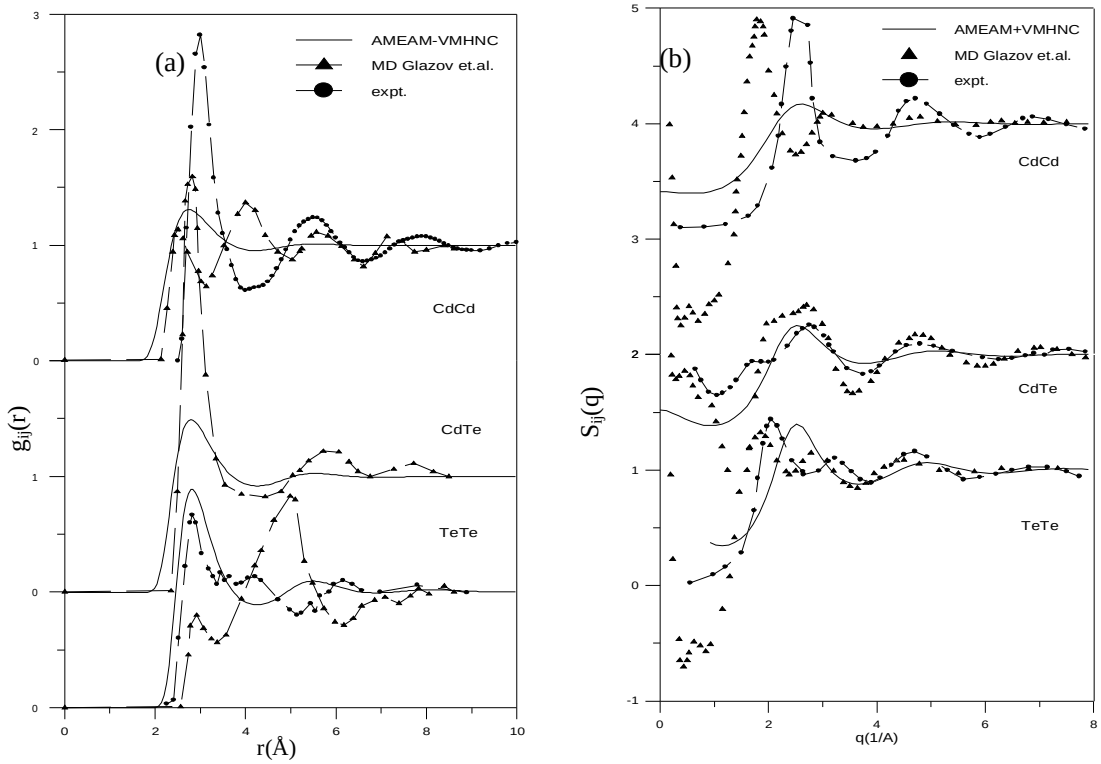


Fig. 6. (a) Partial pair distribution functions and (b) partial structure factors for liquid CdTe alloys.

In Fig. 6, the experimental data for the structure factor of pure Cd and Te are taken from [21]. The pair correlation functions for pure Cd and Te are taken from [34] and [36] respectively. The calculated and experimental curves are similar.

The largest quantitative difference in positions of the minima is observed for Te (lower part in Fig. 6b). Qualitative similarity between Cd-Te partial structure factors and experimental curve is fairly obvious, although the amplitudes are radically different. This shows, in molten CdTe, that CdTe dimers interact with the formation of Te-Te bonds. We also find that the oscillations in our calculated S(q) die out more rapidly than in the experimental data. It is suggested a too soft repulsive potential.

The total pair correlation function, $g_{total}(r)$, and total structure factor, $S_{total}(q)$, for liquid cadmium telluride alloy are plotted in Figs. 7a and 7b, respectively. For comparison, we have also included the experimental data of Gaspard [18]. The $g_{total}(r)$ and $S_{total}(q)$ were determined as a linear combination of corresponding partial ones with the equation given in [17].

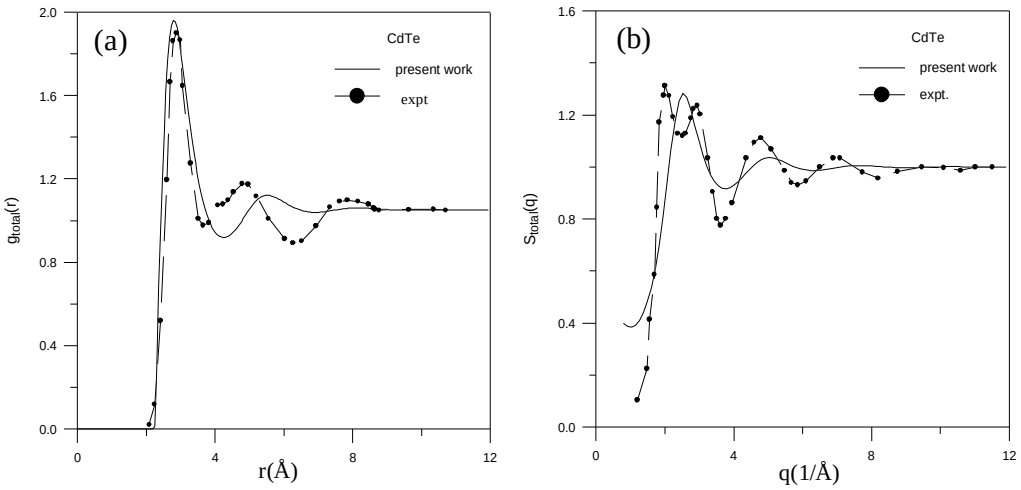


Fig. 7. The calculated total pair correlation functions and structure factors using the AMEAM for liquid CdTe at 1373 K.

The curve in Fig. 7a was used to calculate the coordination number in molten CdTe. We used known formula as, $N = 4\pi\rho\int_0^{r_{min}} r^2 g_{total}(r)dr$ where $r_{min}$ is usually taken to be the position of first minimum in the $g_{total}(r)$ for given temperature, here $r_{min}$ = 4.2 Å. It gives the coordination number as N=6.01. This is very close to more close-packed liquid IV and III-V semiconductors, where the coordination number is ~6. The values obtained from two different experimental data given in [18,21] are 3.3 and 4.4, respectively. The presently obtained coordination number value in combination with the structural properties of liquid CdTe led to, at temperature under consideration, long range order structure of liquid CdTe with found coordination number was retained. Also, it is clear in Fig. 7b that our theoretical result exhibits similar trends with experiment, except in small q region.

## 4. Conclusions

The presented AMEAM provides a realistic description of the pair interaction in liquid CdTe alloys. These calculations were performed with the potential functions that not only fit to solid data but also liquid state properties. We have improved the functional forms of the effective pair potentials in the AMEAM. The structural calculations were carried out using AMEAM derived potentials with the VMHNC theory of liquids. Comparison between the results of the VMHNC theory and available experimental data show that the proposed AMEAM formalism for CdTe alloy systems is capable of providing for the description of its liquid state. The discrepancies between the calculated partial correlations and MD can be observed in small q region. It appears that the SW potential should be reparametrized. The electron density function of the presently proposed AMEAM can be modified for Cd.

## References

[1] M. S. Daw, M. I. Baskes, Phys. Rev. **B29**, 6443 (1984); Phys. Rev. Lett. **50**, 1285 (1983).

[2] M. W. Finnis, J. E. Sinclair, Phil. Mag. **A50**, 45 (1984).
[3] R. A. Johnson, Phys. Rev. B37, 3924 (1988); Philos. Mag. A **63**, 865 (1991).
[4] D. J. Oh, R. A. Johnson, J. Mater. Res. **3**, 471 (1988).
[5] R. A. Johnson, D. J. Oh, J. Mater. Res. **4**, 1195 (1989).
[6] G. J. Ackland, Philos. Mag. A **66**, 917 (1992).
[7] G. J. Ackland, S. J. Wooding, D. J. Bacon, Philos. Mag. A **71**, 553 (1995).
[8] M. I. Baskes, R. A. Johnson, Modelling Simul. Mater. Sci. Eng. **2**, 147 (1994).
[9] R. Pasianot, E. J. Savino, Phys. Stat. Sol. (b), 176 (1993).
[10] W. Hu, B. Zhang, B. Huang, F. Gao, D.J. Bacon, J. Phys.: Condens. Matter. **13**, 1193 (2001).
[11] M. I. Baskes, Phys. Rev. **B46**, 2727 (1992).
[12] S. Chen, J. Xu, H. Zhang, Comp. Mat. Sci **29**,428 (2004).
[13] W. Hu, M. Fukumoto, Modelling Simul. Mater. Sci. Eng. **10**, 707 (2002).
[14] W. Hu, H. Xu, X. Shu, X. Yuan, B. Gao, B. Zhang, J. Phys. D: Appl. Phys. **33**, 711 (2000).
[15] W. Hu, H. Deng, X. Yuan, M. Fukumoto, Eur. Phys. J. **B34**, 429 (2003).
[16] V. V. Godlevsky, J. J. Derby, J. R. Chelikowsky, Phys. Rev. Lett. **81**, 4959 (1998).
[17] V. V. Godlevsky, M. Jain, J. J. Derby, J. R. Chelikovsky, Physical Rev. **B60**, 8640 (1999).
[18] J. P. Gaspard, C. Bergman, C. Bichara, R. Bellisent, P. Chieux, J. Goffard, J. Non-Cryst Solids **97/98**, 1283 (1987); J. P. Gaspard, J. Raty, R. Ceolin, R. Bellisent, J. Non-Cryst Solids **205-207**, 75 (1996).
[19] Z. Q. Wang, D. Stroud, A. J. Markworth, Phys. Rev. **B40**, 3129 (1989).
[20] F. H. Stillinger, T. A. Weber, Phys. Rev **B31**, 5262 (1985).
[21] V. M. Glazov, L. M. Pavlova, Scandinavian J. Metall. **31**,52 (2002).
[22] L. E. Gonzalez, D. J. Gonzalez, M. Silbert, Physica **B168**, 39 (1991); L. E. Gonzalez, D. J. Gonzalez and M. Silbert, Phys. Rev. **A45**, 3803 (1992);
[23] L. E. Gonzalez, D. J. Gonzalez, S. Dalgic, M. Silbert, Z. Phys. **B103,** 13 (1997).
[24] S. S. Dalgıc, S. Dalgıc, G. Tezgor, Phys. Chem. Liq. **40**, 539 (2002).
[25] G. M. Bhuiyan, M. Silbert, M. J. Stott, Phys. Rev. **B 53**, 636 (1995).
[26] G. M. Bhuiyan, M. A. Khaleque, J. Non – Cryst. Solids, **226**, 175 (1998).
[27] M. M. G. Alemany, C. Rey, L. J. Gallego, Phys. Rev. **B 58**, 685 (1998).
[28] S. S. Dalgic, S. Dalgic, U. Domekeli, J. Optelectron. Adv. Mater. **5**, 1263 (2003).
[29] B. W. Zhang, Y. F. Ouyang, Z. Phys. **B92**, 431 (1993).
[30] J. H. Rose, J. R. Smith, F. Guinea, J. Ferrante, Phys. Rev. **B29**, 2963 (1984).
[31] R. A. Johnson, Phys. Rev **B39**, 12554 (1989).
[32] T. Iida, R. I. L. Guthrie, The Physical Properties of Liquid Metals (Clarendon Press, Oxford, 1993).
[33] C. Kittel, Introduction to Solid State Physics, 6th edition (1986).
[34] Y.Waseda, The Structure of Non-Crystalline Materials-Liquids and Amorphous Solids (McGraw-Hill, New York, 1981).
[35] N. W. Ashcroft, D. C. Langreth, Phys. Rev. **159**, 500 (1967).
[36] K. Sefier-Lorenz, G. Kresse, J. Hafner, J. Non-Cryst Solids **312-314**, 371 (2002).